THE UNIVERSITY OF MICHIGAN

College of Engineering
Department of Mechanical Engineering
Cavitation and Multiphase Flow Laboratory

Report No. UMICH 03371-17-T

ON THE EROSION RATE - DROPLET SIZE RELATION FOR AN EXPERIMENTAL STAND WITH A ROTATING SAMPLE

by

J. Krzyžanowski*

Typing and reproduction supported by:
National Science Foundation
Grant No. GK-730

May, 1972

*Presently on leave as Visiting Scientist from the Institute of Fluid Flow Machinery of the Polish Academy of Sciences, Gdańsk, Poland.

ABSTRACT

There is still little known about the droplet size-erosion rate patterns for wet steam turbine stages. It has been already proved that the structure of the droplet stream may influence very much some of the impact parameters governing the erosion of the turbine blading (ref. 1). In order to shed more light on the problem, a series of experiments was initiated at IFFM.* In the test stand of IFFM the structure of the droplet stream may be readily controlled. The aim of this report is to present the algorithm relating the structure of the droplet stream in the mentioned stand with some impact parameters. Also an attempt is made toward preliminary evaluation of the experimental results presented in (ref. 3).

---

*Institute of Fluid Flow Machinery of the Polish Academy of Sciences, Gdansk, Poland.

TABLE OF CONTENTS

1. NOMENCLATURE

$A' = \sqrt{\dfrac{0.85\ \mu\ \rho}{r_*^3\ \rho_*^2\ c_1}}$

c_1 air velocity, m/s

c_* droplet velocity, m/s

D mean diameter of the rotor, m

D_s mean diameter of the sample, m

$E \equiv \dfrac{y_o}{D_s/2}$ coefficent of droplet separation

E_r rationalized erosion rate

F see Fig. 3, m

G constant, m^3/s

$f_n \equiv \dfrac{1}{\Delta r_*} \dfrac{n(r_*, c_1)}{N}$ number distribution function, 1/m

k factor of proportionality, see Fig. 4, mg/m

L see Fig. 3, m

$n\ (r_*, c_1)$ number of the droplets of a given size r_* per unit area

N number of all droplets per unit area

N_a normalized erosion resistance

$N_{1,2,3}$ constants

r_* droplet radius, m

u circumferential velocity, m/s

U_a water flux over the sample surface, $m^3/m^2 s$

UA see (18) and (B7)

$\bar{U}_a$ mean value of U_a, $m^3/m^2 s$

$\overline{UA}$ see (19) and (B9)

U_{eM} maximum instantaneous value of the volumetric material less per unit area and unit time m^3/m^2s

UEM see (23) and (B11)

$\overline{U}_{eM}$ mean value of U_{eM}, m^3/ms

$\overline{UEM}$ see (24) and (B12)

w_* droplet's velocity in the relative frame of reference, m/s

w_{*N} normal component of w_*, m/s

$\overline{w}_{*N\,AR}$, $\overline{\overline{w}}_{*N\,AR}$, $\overline{w}_{*N\,M}$, $\overline{\overline{w}}_{*N\,M}$ mean values of w_{*N}, m/s

w_1 air velocity in the relative frame of reference, m/s

α, γ see Fig. 2, ^{o}

Δm loss of material eroded, mg

ΔM_* amount of water supplied onto the trailing edge of the flat plate per its length ΔR_1, kg/s

ΔR_1 the length element of the trailing edge of the flat plate, m

$\Delta(\Delta m)/\Delta\tau$ the maximum slope of the curve $\Delta m = f(\tau)$, mg/min.

κ parameter , see (B1)

μ viscosity of air, kg/ms

φ, φ_n see Fig. 3, ^{o}

φ_m see Fig. 8, ^{o}

ρ density of air, kg/m^3

ρ_* density of water, kg/m^3

τ time, minutes

2. INTRODUCTION

There are some characteristic features of the kinematics of a droplet motion in the axial gap of a steam turbine blading.

The neighborhood of the leading edge of the rotor blade is exposed to the impact of droplets whose radius is a function of the location of the blade surface element. The further away from the leading edge of the blade the surface element is located, the smaller are the maximum and mean value of the droplet radius. Also the angle of attack, which is a function of the inclination of the blade surface element and the droplet size, changes.

Another characteristic feature of the droplet impact intensity is its strong dependence upon the structure of the droplet stream. This had been proved in (ref. 1), where the correlation between droplet stream structure and the impact parameters was considered.

In the experimental investigation of the material removal-time patterns for different material, these characteristic features of the droplet stream are usually not taken into account:

1. The droplets, no matter what their size, collide with the sample of the material under the same angle of attack. Usually this angle is 90 degrees.
2. The structure of the droplet stream is usually relatively homogeneous. In general, little is known about this structure and often not even the droplet stream is used in tests, but rather a liquid jet.

It appears, however, that both the angle of attack and the droplet structure have substantial influence upon erosion rate patterns. As far as the influence of the angle of attack is concerned, some information is already available. One comes roughly to the conclusion that the normal component of the impact velocity governs the erosion.* Much less is known about the influence of the droplet size. Only recently (ref. 2) an attempt was made to draw some preliminary conclusions from the meager experimental data; it is there assumed that the drop size effect can be represented by a factor of the form

$$w_{*N}^{2} \, r_{*} = \text{const}$$

where the constant represents a critical or threshold combination of velocity and droplet size, such that, for $w_{*N}^{2} \, r_{*} \leqslant$ constant no significant erosion occurs.

In order to shed more light on the droplet size effect, among others, a test rig with rotating sample was built in the Institute of Fluid Flow Machinery of the Polish Academy of Sciences. The sample intersects once per rotation the droplet stream generated in the aerodynamic wake of a flat plate. The particular feature of the stand is that the droplet stream structure may readily be controlled by changing the air velocity in the test section, the amount of water per unit time and unit width of the plate, the length of the plate, the shape of the trailing edge of the plate, etc. Mr. B. Weigle designed the stand; he and Mr. H. Severin are in charge of the

*See extensive reference data in (ref. 2).

experiments. The outline of the stand is shown in Fig. 1. More details are available elsewhere, (ref. 3).

The aim of this report is to present the algorithm relating the structure of the droplet stream with mean values of some selected impact parameters. The structure of the droplet stream is defined by the droplet size distribution function. This function is assumed to be known, and to depend upon the droplet size and air velocity. Particular attention is paid to the mean value of the amount of water impinging upon the unit area of the sample per unit time, the mean value of the product of this amount of water and $(w_{*N}/2550)^5$, and the mean value of the impact velocity. A preliminary evaluation of the experimental results presented in (ref. 3) is made.

3. FORMULATION

Before we formulate the conditions of the droplet impact with the rotating sample of the IFFM experimental stand, let us consider the kinematics of the individual droplet.

In some prior authors' papers, it has been indicated that the droplet motion in the aerodynamic wake may be described with sufficient accuracy by the equation:

$$\frac{c_*}{c_1} = 0.8\left\{1 - \frac{1}{[1 + A'z + \sqrt{A'^2z^2 + 2A'z}]^2}\right\} \tag{1}$$

c_* is the droplet velocity in the absolute reference frame of coordinates. The relationship between this velocity, the gas velocity, and droplet size is shown in Fig. 2. The group of parameters is relevant to the IFFM stand. The droplet velocity w_* in the relative reference frame of coordinates:

$$\vec{w}_* = \vec{c}_* - \vec{u} \tag{2}$$

and the droplet path in this reference frame are also shown.

The conditions of the droplet impact may be easily calculated under the assumption that the droplet path shown in Fig. 2 does not change its shape in the neighborhood of the sample. This assumption has been evaluated in Appendix B in more detail.

Let us now consider first the amount of water which hits the unit area of the sample per unit time. This parameter of the droplet impact is worth considering because it has been already shown that the erosion rate is proportional to it. Let us assume that the structure of the droplet stream is defined by the droplet size distribution function

$$f_n(r_*, c_1) \equiv \frac{1}{\Delta r_*} \frac{n(r_*, c_1)}{N} \tag{3}$$

and that this function in the point where the sample intersects the droplet stream is given by the equation

$$f_n(r_*, c_1) = N_1 \, r_*^{N_2} \, e^{-N_3 r_*} , \quad N_1, N_2, N_3 = f(c_1) \tag{4}$$

Then the number of droplets of a particular size r_* impinging upon the surface element $\Delta R_1 \cdot \frac{D_s}{2} \cdot d\varphi$ of the sample per one crossing of the droplet stream is equal to

$$n(r_*, c_1) \, L \cdot F = n(r_*, c_1) \, L \cdot \frac{D_s}{2} \, d\varphi \, \sin\varphi \, \frac{1}{\cos\alpha(r_*, c_1)} \tag{5}$$

The volume of the water carried by these droplets is equal to

$$\frac{4}{3} \Pi \, r_*^3 \cdot n(r_*, c_1) \, L \, \frac{D_s}{2} \, d\varphi \, \sin\varphi \, \frac{1}{\cos\alpha(r_*, c_1)} \tag{6}$$

since

$$\cos\alpha(r_*, c_1) = \frac{u \sin\gamma}{w_*(r_*, c_1)} \tag{7}$$

and the frequency with which the sample crosses the droplet stream per unit time is $u/\pi D$. Hence, the volumetric flux relevant to this volume of water is equal to

$$\delta U_a(r_*, c_1, \varphi) = \frac{4}{3} \Pi \, r_*^3 \cdot LN \, f_n(r_*, c_1) \Delta r_* \, \frac{w_*(r_*, c_1) \sin\varphi}{u \sin\gamma} \cdot \frac{u}{\Pi D} \cdot \frac{1}{\Delta R_1} \tag{8}$$

The product LN may be eliminated by means of the continuity equation for the liquid phase formulated for the cross-section 0-0 of the droplet stream. It has the form: $\Delta M_* = \sum_{r_*=o}^{\infty} L\ c_*(r_*,c_1)\ n\ (r_*) \cdot \frac{4}{3}\Pi\ r_*^3 \cdot \rho_*$

$$= \sum_{r_*=o}^{\infty} L\ c_*(r_*,c_1)\ f_n(r_*,c_1)\ N\ \Delta r_*\ \frac{4}{3}\Pi\ r_*^3\ \rho_* \qquad (9)$$

The sumation, which may be replaced by integration is extended over all the droplet radii in the stream. Instead of Eq. (9), one may write:

$$\Delta M_* = \frac{4}{3}\Pi\ \rho_*\ LN \int_o^{\infty} r_*^3\ f_n(r_*,c_1)\ c_*(r_*,c_1)\ dr_* \ . \qquad (10)$$

Hence

$$LN = \frac{\Delta M_*}{\frac{4}{3}\Pi\ \rho_* \int_o^{\infty} r_*^3\ f_n(r_*,c_1)\ c_*(r_*,c_1)\ dr_*} \qquad (11)$$

For the particular droplet size the angle $\alpha\ (r_*, c_1)$ may be expressed by the equation:

$$\alpha = \text{arc}\ \tan\alpha \qquad (12)$$

where

$$\tan\alpha = \text{sign}\left[\sin\left(\frac{c_*(r_*,c_1) - u\cos\gamma}{w_*(r_*,c_1)}\right)\right] \cdot \frac{w_*(r_*,c_1)}{u\cdot\sin\gamma}\sqrt{1-\frac{u^2\sin^2\gamma}{w_*^2(r_*,c_1)}} \qquad (13)$$

The sign-function takes care of the appropriate sign of term tan α . The second part of the R-H-S of the Eq. (13) may be easily deduced from the geometric relationship shown in Fig. 2. It must be remembered that for each droplet size r_*, we obtain a different α or, in other words, $\alpha = \alpha\,(r_*, c_1)$. Hence, in order to validate the Eq. (8) for all droplet sizes, the $\sin\varphi$ function in it must be replaced by function $F(\varphi)$, such that (see fig. 3):

$$F(\varphi) = 0 \qquad \text{for } \varphi < \varphi_n(r_*,c_1) - \frac{\Pi}{2}$$

$$F(\varphi) = \overline{\sin}\,[\varphi - \varphi_n(r_*,c_1) + \frac{\Pi}{2}] \quad \text{for } \varphi_n(r_*,c_1) - \frac{\Pi}{2} \leq \varphi \leq \varphi_n(r_*,c_1) + \frac{\Pi}{2}$$

$$F(\varphi) = 0 \qquad \text{for } \varphi > \varphi_n(r_*,c_1) + \frac{\Pi}{2} \qquad (1\ )$$

where:

$$\varphi_n(r_{*i},c_1) = \varphi_n(r_{*i-1},c_1) + \alpha(r_{*i-1},c_1) - \alpha(r_{*i},c_1) \qquad (15)$$

$i = 1, 2, 3, \ldots\ldots\ldots,$

also,

$$\varphi_n(r_{*o},c_1) = \frac{\Pi}{2} \text{ and } \alpha(r_{*o},c_1) = \alpha(r_{*1},c_1) \qquad (16)$$

Rearranging (8) by means of (11) and (14) results in

$$\delta U_a(r_*,c_1,\varphi) = \frac{1}{\rho_*} \cdot \frac{\Delta M_*}{\Delta R_1} \frac{r_*^3 f_n(r_*,c_1)}{\int_0^\infty r_*^3 f_n(r_*,c_1)\, c_*(r_*,c_1)\, dr_*} \cdot \frac{w_*(r_*,c_1)}{\Pi D_s \sin\gamma} \cdot \overline{\sin}\,[\varphi - \varphi_n(r_*,c_1) + \frac{\Pi}{2}]\Delta r_* \qquad (17)$$

One establishes the volumetric water flux $U_a(c_1, \varphi)$ for a surface element located by φ extending the integration of the value $\delta U_a(r_*, c_*, \varphi)$ over the whole range of droplet size. Hence one finally obtains:

$$U_a(c_1,\varphi) = \frac{1}{\rho_*} \frac{\Delta M_*}{\Delta R_1} \frac{1}{\Pi\, D_s \sin\gamma} \int_0^\infty \frac{r_*^3\, f_n(r_*,c_1)\, w_*(r_*,c_1)}{\int_0^\infty r_*^3\, f_n(r_*,c_1)\, c_*(r_*,c_1)\, dr_*} \cdot$$

$$\overline{\sin}\,[\varphi - \varphi_n(r_*,c_1) + \frac{\Pi}{2}]\, dr_* = \frac{1}{\rho_*} \frac{\Delta M_*}{\Delta R_1} \frac{1}{\Pi\, D_s \sin\gamma}\, UA(c_1,\varphi) \qquad (18)$$

In order to eliminate the dependence of φ one may average $U_a(c_1, \varphi)$ over the circumference of the sample. Hence:

$$\overline{U}_a(c_1) = \frac{1}{\varphi_n(r_{*max},c_1) + \frac{\Pi}{2}} \frac{\frac{1}{\rho_*} \frac{\Delta M_*}{\Delta R_1} \frac{1}{\Pi\, D_s \sin\gamma}}{\int_0^\infty r_*^3\, f_n(r_*,c_1)\, c_*(r_*,c_1)\, dr_*} \cdot \int_0^{\varphi_n(r_{*max},c_1) + \frac{\Pi}{2}}$$

$$\int_0^\infty r_*^3\, f_n(r_*,c_1)\, w_*(r_*,c_1)\, \overline{\sin}\,[\varphi - \varphi_n(r_*,c_1) + \frac{\Pi}{2}]\, dr_*\, d\varphi$$

$$= \frac{1}{\rho_*} \frac{\Delta M_*}{\Delta R_1} \frac{1}{\Pi\, D_s \sin\gamma}\, \overline{UA}(c_1) \qquad (19)$$

The erosion rate is obviously not only the function of the flux of water impinging upon the surface element of the rotating sample. It is also a function of the impact velocity. This relationship may be expressed as an empirical equation in the form (ref. 4):

$$\frac{\Delta m}{\tau} = k \frac{U_a}{N_a} \left(\frac{w_{*N}}{2550}\right)^5 \exp(-0.25\, \Delta m/\Delta m_T) \qquad (20)$$

For a flat sample the coefficient $k = F \cdot \rho$. Other symbols of Eq. (20) are explained on Fig. 4. The maximum instantaneous erosion rate $\frac{\Delta(\Delta m)}{\Delta\tau}$ is according to (ref. 4) and Eq. (20) equal to:

$$\frac{\Delta(\Delta m)}{\Delta\tau} = k \frac{U_a}{N_a}\left(\frac{w_{*N}}{2550}\right)^5 \equiv U_{eM} \qquad (21)$$

Here U_{em} represents the maximum instantaneous value of erosion rate. These empirical relationships have been established for the flat material sample attacked by a relatively homogeneous (in size and direction) droplet stream. Application of these formulae for the case of cylindrical, rotating samples demands assuming that the erosion damage caused by the droplet groups of a particular size may be superimposed. That assumption has not yet been proved and may be accepted here merely as a first approximation. Under this assumption, the theoretical evaluation of the maximum instantaneous value of erosion rate may be based on the value:

$$\delta U_{eM}(r_*,c_1,\varphi) = \delta U_e(r_*,c_1,\varphi) \cdot \left(\frac{w_{*N}(r_*,c_1,\varphi)}{2550}\right)^5 \qquad (22)$$

its integral extended over all droplet size:

$$U_{eM}(c_1,\varphi) = \int_0^\infty \delta U_{eM}\, dr_* = \frac{1}{\rho_*}\frac{\Delta M_*}{\Delta R_1}\frac{1}{\Pi D_s \sin\gamma}\int_0^\infty \frac{r_*^3 f_n(r_*,c_1)\, w_*(r_*,c_1)}{\int_0^\infty r_*^3 f_n(r_*,c_1)\, c_*(r_*,c_1)dr_*} \cdot$$

$$\cdot \left[\frac{w_{*N}(r_*,c_1,\varphi)}{2550}\right]^5 \overline{\sin}\, [\varphi - \varphi_n(r_*,c_1) + \frac{\Pi}{2}]\, dr_*$$

$$= \frac{1}{\rho_*}\frac{\Delta M_*}{\Delta R_1}\frac{1}{\Pi D_s \sin\gamma} \cdot UEM(c_1,\varphi) \qquad (23)$$

and the mean value:

$$\overline{U}_{eM}(c_1) = \frac{1}{\varphi_n(r_{*max},c_1) + \frac{\Pi}{2}} \int_0^{\varphi_n(r_{*max},c_1) + \frac{\Pi}{2}} U_{eM}(c_1,\varphi)\, d\varphi =$$

$$= \frac{1}{\varphi_n(r_{*max},c_1) + \frac{\Pi}{2}} \; \frac{\frac{1}{\rho_*} \frac{\Delta M_*}{\Delta R_1} \frac{1}{\Pi\, D_s \sin\gamma}}{\int_0^{\infty} r_*^3 f_n(r_*,c_1)\, c_*(r_*,c_1)\, dr_*} \cdot \int_0^{\varphi_n(r_{*max},c_1) + \frac{\Pi}{2}}$$

$$\int_0^{\infty} r_*^3 f_n(r_*,c_1)\, w_*(r_*,c_1) \left[\frac{w_{*N}(r_*,c_1,\varphi)}{2550}\right]^5$$

$$\overline{\sin}\,[\varphi - \varphi_n(r_*,c_1) + \frac{\Pi}{2}]\, dr_*\, d\varphi = \frac{1}{\rho} \frac{\Delta M_*}{\Delta R_1} \frac{1}{\Pi\, D_s \sin\gamma}\, \overline{UEM}(c_1) \qquad (24)$$

The relevant programs of numerical calculations of these impact parameters are presented in Appendix A and B. In Appendix B, in addition, the equations for local and mean value of the impact velocity are given.

4. SOME RESULTS OF NUMERICAL CALCULATION AND SOME EXPERIMENTAL RESULTS

The theoretical analysis presented in the previous section and in Appendix B had been triggered by interesting experimental results of B. Weigle and H. Severin (ref. 3). They had found that for constant mass flux of water, G_w, supplied per unit width per unit time onto the plate, for constant circumferential velocity, u, of the sample but changing gas velocity c_1 in the range of

$$c_1 = 60 \frac{m}{s} \text{ through } 75, 92, 153 \frac{m}{s},$$

the erosion rate changes substantially. A fragment of the experimental results in the form of the relation $\Delta m = f(\tau)$ is shown in Fig. 5. There is also shown the droplet size distribution functions relevant to the gas velocity c_1. It is apparent that with the increase of gas velocity c_1 the dispersion of the droplets increases, and the representative mean value of the droplet size

$$r_{*m} = \int_0^\infty r_*^3 f_n(r_*, c_1) \, dr_* \tag{25}$$

decreases, as does the erosion rate represented by the ratio $\Delta(\Delta m)/\Delta\tau$ defined in Fig. 4.

This significant change in erosion rate may be a result from several different effects. One of these may be the change in amount of water impacting the sample per unit area and unit time. As a matter of fact, Heymann's empirical relation (Eq. 20) says that the maximum instantaneous value of erosion rate $\Delta(\Delta m)/\Delta\tau \cong U_{em}$ is proportional to the volumetric water flux U_a over the eroded surface of the sample. The other reason for the change of experimental value of $\Delta(\Delta m)/\Delta\tau$ may be the change in the term $U_a\left(\frac{w_{*N}}{2550}\right)^5$. It is also proportional to $\Delta(\Delta m)/\Delta\tau$

Numerical calculation presented in this section have been performed for the following set of parameters relevant to the stand of IFFM:

c_1 = 60, 75, 92, 153 m/s

u = 200 m/s

γ = 80^o

D_s = $7\cdot 10^{-3}$ m

Δr_* = $10 \cdot 10^{-6}$ m

μ = $1.85 \cdot 10^{-5}$ kg/ms

ρ = 1.205 kg/ms

ρ_* = 1000 kg/ms

z = 0.3 m

In Fig. 6 the results of numerical calculations of $\overline{UA}$ and $\overline{UEM}$ are presented. Both $\overline{UA}$ and $\overline{UEM}$ are proportional to $\overline{U}_a$ and $\overline{U}_{eM}$ respectively (see Eq. 19, 24). $\overline{UA}$ and $\overline{UEM}$ decrease, as does the experimental value $\Delta(\Delta m)/\Delta\tau$ when c_1 increases. The trend of change of both theoretical and experimental values is the same. However, it may be readily shown that

$$\left(\frac{\Delta(\Delta m)}{\Delta\tau}\right)_{c_1} \Big/ \left(\frac{\Delta(\Delta m)}{\Delta\tau}\right)_{c_1 = 75\ m/s}$$

changes much faster than do $UA_{C_1} / UA_{C_1=75}$ and $UEM_{C_1}/UEM_{C_1=75}$.

For c_1 = 153 m/s there is already a difference in order of magnitude between the theoretical and experimental values. This difference clearly may not be explained as the consequence of averaging, or the assumption concerning the superposition of erosion caused by the droplet groups of particular size.

In searching for a reason for this discrepancy, attention must be paid to the problem of the correlation between the droplet stream structure and the erosion rate pattern. The program of experiments of B. Weigle and M. Severin is particularly suitable for these investigations because their stand makes it possible to change the droplet stream structure easily for almost unchanged mean impact velocity (Fig. 6).

Little is known, however, about the droplet size-erosion rate relationship, and only in exceptional experiments was the droplet size investigated. However, it has been indicated (ref. 2) that the droplet size is probably related to the maximum instantaneous value of rationalized erosion rate, through the influence on its threshold value. The rationalized erosion rate has been defined in (ref. 2) as follows:

$$E_r = \frac{\text{Volume of material lost per unit area per time}}{\text{Volume of liquid impinged per unit area per unit time}}$$

In the nomenclature of this report:

Volume of material lost per unit area per unit time =

$$= \Delta(\Delta m) \frac{1}{\rho_s} \Big/ \Delta\tau \cdot L$$

and Volume of liquid impinged per unit area per unit time =

$$= \overline{U}_a = \frac{1}{\rho_*} \frac{\Delta M_*}{\Delta R_1} \frac{1}{\Pi D_s \sin\gamma} \overline{UA}$$

Hence

$$E_r(c_1) \sim \frac{\Delta(\Delta m)/\Delta\tau}{\overline{UA}}$$

In Ref. 2 Heymann suggests the droplet size-erosion rate dependence in the form of the following possible relations:

$$E_r = f_1\left[w_{*N}\left(1 - \frac{G}{w_{*N}^2\, r_*}\right)\right] \quad \text{or} \quad E_r = f_2\left[w_{*N} - \sqrt{\frac{G}{r_*}}\right] \tag{26}$$

For both of these relations, which strictly speaking, are not yet fully confirmed by experiment, the terms $\frac{G}{w_{*N}^2\, r_*}$ and $\sqrt{G/r_*}$ relate to the threshold impact velocity w_{*Nc} such that for $w_{*N} \leq w_{*Nc}$ no erosion results. G may be considered as a material constant. Now, the experimental data of (ref. 3) for an aluminum sample, partially quoted in Fig. 5, may be used to determine this constant G, and thus the relationship between w_{*Nc} and r_*. It may be done by means of the plot $E_r = f(r_*)$ because in the experiments mentioned, the mean value of the impact velocity w_{*N} was almost constant. In fact, for $u = 200$ m/s the mean impact velocity changes only between

$$\bar{\bar{w}}_{*N} = 119;\ 117.1;\ 115.5 \text{ and } 113.5 \text{ m/s}$$

for

$$c_1 = 60;\ 75;\ 92 \text{ and } 153 \text{ m/s respectively.}$$

Thus, from the appropriate extrapolation of the function $E_r = f(r_*)$ (see Fig. 7), for a given impact velocity $\bar{\bar{w}}_{*N} = \sim 116$ m/s, results the threshold droplet size $r_{*c} = 44.10^{-6}$ m. Hence, for the material considered

$$G = d_{*c} \cdot \bar{\bar{w}}_{*N}^2 = 1{,}185 \frac{m^3}{s^2}$$

The relation $w_{*Nc} = f(r_*)$ for an aluminum sample used in (ref. 3) is shown in the Fig. 6. The results of the Busch and Hoff experiments (ref. 2) may be here recollected. They obtained for the rain-eroded aluminum the threshold velocity $w_{*Nc} = \sim 33$ m/s. Hence, the corresponding droplet size d_* would be the order 1.10^{-3} m which appears qualitatively reasonable for the rain droplet size.

It has to be pointed out here that in this report only a small part of the results of (ref. 3) has been used. In addition, in assessment of r_{*c} and G, the results for only one velocity w_{*N} have been used. More extensive experimental data are needed to shed more light on the problem. As far as the author is informed, the program of relevant experiments is being continued in IMMF.

5. CONCLUSIONS

1. The experimental investigation of B. Weigle and H. Severin, published in (ref. 3), indicated substantial dependence of the derosion damage-time patterns upon the droplet size.

2. These experimental results of IFFM deserve certainly some more consideration. To make it possible, a theoretical model of droplet impact for the experimental stand of IFFM has been presented in this report. Attention has been particularly paid to the calculations of the mean value of the volumetric water flux U_a over the sample surface. Also the mean value of the product of water flux, U_a, and $(\frac{w_{*N}}{2550})^5$ as well as the mean impact velocity w_{*N} have been calculated.

3. Comparison of experimental and theoretical data indicated that the experimentally established rationalized erosion rate, E_r, changes faster with the gas velocity c_1 than theoretically calculated water flux $\bar{U}_a$ and the mean value $\bar{\bar{U}}_{eM}$ of the product $U_a \left(\frac{w_{*N}}{2550}\right)^5$.

4. It is likely that variation in droplet size causes this discrepancy. The threshold droplet size of order $r_* = \sim 44.10^{6}$ m for mean impact velocity $\bar{\bar{w}}_{*N} = \sim 116$ m/s for soft aluminum has been established under the assumption (ref. 2) that the droplet size effect can be represented by a factor of the form:

$$w_{*N}^2 \, r_* = \text{const} = 1/G$$

5. The model presented of the droplet impact indicated that the experimental stand of IFFM is particularly suitable for experiments designed to shed more light on the problem of droplet size effect:

5.1 It provides the possibility of the exceptional change of the mean dropl size between $r_* = \sim 50.10^{-6}$ m up to about $r_* = \sim 300.10^{-6}$ m.

5.2 The mean value of the impact velocity may be controlled independently.

5.3 The droplet stream structure seems to approach the stream structure in the steam turbine.

6. Further investigation of the relationship between the erosion resistance and the droplet size are of importance because in (ref. 1) it has been already shown that the impact parameters are also seriously influenced by the droplet stream structure. Thus the control of the droplet stream

structure may offer a powerful method for the protection of steam turbine blading.

6. ACKNOWLEDGMENTS

This report has been prepared during the author's sabbatical year in the United States, which was arranged in the exchange program between the Polish Academy of Sciences, Warsaw, and the National Academy of Sciences, Washington, D. C. The author appreciates the assistance of his hosts in the United States: Professor J. R. Moszynski of the University of Delaware and Professor F. G. Hammitt of the University of Michigan. The author is also indebted to his colleagues Mr. B. Weigle and Mr. H. Severin for supplying some of their experimental results before publication (ref. 3). Finally, the author is grateful to Mr. Frank J. Heymann for numerous discussions which stimulated preparation of this report.

7. APPENDICES

APPENDIX A

The program of numerical calculations has been formulated in Algol for the Burroughs B 5500 computer. The text of the program is quoted below. It makes it possible to calculate:

$$\varphi_n(r_*, c_1),\ \alpha(r_*, c_1),\ r_{*m}(c_1),\ \varphi_n(r_{*max}, c_1),$$

$$UA(c_1,\varphi),\ UEM(c_1,\varphi),\ \overline{UA}(c_1),\ \overline{UEM}(c_1)$$

according to the equation (15), (12), (25), (15), (18), (23), (19), and (24), respectively.

The input data have to be sequenced according to the sequence numbers: 900 and 1000 where:

$c_1 \equiv C_1$, $u \equiv U$, $\gamma \equiv GAMA$, $\Delta r_* \equiv DR$, $\mu \equiv MI$, $\rho \equiv RO$,

$\rho_* \equiv RO_1$, $z \equiv Z$, $N_1 \equiv N11$, $N_2 \equiv N22$, $N_3 \equiv N33$

The output data are being printed in the sequence resulting from sequence numbers: 2350, 2500, 5050, and 5800 where:

$r_* \equiv R[K]$, $\varphi_n(r_*, c_1) \equiv FINDGR[K]$, $\alpha(r_*, c_1) \equiv ALFADGR[K]$, $r_{*m} \equiv J[51]$,

$\varphi_n(r_{*max}, c_1) + \frac{\Pi}{2} \equiv FIMAXDGR$, $\Delta\varphi \equiv \dfrac{\varphi_n(r_{*max}, c_1) + \Pi/2}{N_{max} - 1} \equiv DELTAFIDGR$,

N, $\varphi(N) \equiv FIDGR[N]$, $UA(c_1,\varphi) \equiv UA[N]$, $UEM(c_1,\varphi) \equiv UEM[N]$,

$\overline{UA}(c_1) \equiv UASR[N_{max}]$, $\overline{UEM}(c_1) \equiv UEMSR[N_{max}]$.

```
100  BEGIN
200  COMMENT BADANIE UA,UEM DLA WIRUJACEJ PROBKI W FUNKCJI C1 (WAR II);
300  REAL C1,U,GAMA,N11,N22,N33,DR,MI,RO,RO1,Z,CALKA1,CALKA2,
350        FIMAX,DELTAFI,FIMAXDGR,DELTAFIDGR,CALKA3,CALKA4,
360         CALKA5,CALKA6;
400  INTEGER K,N;
500  LABEL ET1;
600  ARRAY R,FN,A1,CKR,H,I,G,J,L,WKR,M,O,UA,P,UEM,
650         TGALFA,ALFA,FIN,ALFADGR,FINDGR,WKRN[1:51],
660         A3,A4,UASR,UEMSR,FI,FIDGR[1:21];
700  FILE JAK33 REMOTE(2,9);
800  FORMAT FORMAT1 (5E14.3);
850  FORMAT FORMAT2(X1);
900  ET1: READ(JAK33,/,C1,U,GAMA,DR,MI,RO,RO1,Z);
1000 READ (JAK33,/,N11,N22,N33);
1010 CALKA1:=0;
1020 CALKA2:=0;
1100 K:=2;
1200 R[K-1]:=0;
1205 G[K-1]:=0;
1210 H[K-1]:=0;
1220 I[K-1]:=0;
1230 J[K-1]:=0;
1300 FOR K:=2 STEP 1 UNTIL 51 DO
1400  BEGIN
1500    R[K]:=R[K-1]+DR;
1600    FN[K]:=N11\R[K]*N22\EXP(-N33\R[K]);
1700    A1[K]:=SQRT((.85\MI\RO)/(R[K]*3\RO1*2\C1));
1800    CKR[K]:=.8\C1\(1-1/(1+A1[K]\Z+
1900            SQRT(A1[K]*2\Z*2+2\A1[K]\Z))*2);
1910    WKR[K]:=SQRT(U*2\(SIN(GAMA))*2+(CKR[K]-U\COS(GAMA))*2);
2000    G[K]:=R[K]*3\FN[K];
2050    H[K]:=R[K]*3\CKR[K]\FN[K];
2055     O[K]:=R[K]*3\WKR[K]\FN[K];
2100    CALKA1:=(H[K-1]+H[K])/2\DR;
2200    I[K]:=I[K-1]+CALKA1;
2300    CALKA2:=(G[K-1]+G[K])/2\DR;
2310    J[K]:=J[K-1]+CALKA2;
2320    TGALFA[K]:=SIGN(SIN((CKR[K]-U\COS(GAMA))/WKR[K]))\
2323              WKR[K]/(U\SIN(GAMA))\SQRT(1-U*2\(SIN(GAMA))*2/
2326              WKR[K]*2);
2330    ALFA[K]:=ARCTAN(TGALFA[K]);
2333    IF K EQL 2
2336       THEN FIN[K]:=1.570796
2339       ELSE FIN[K]:=FIN[K-1]+ALFA[K-1]-ALFA[K];
2340    ALFADGR[K]:=ALFA[K]\360/6.283185;
2345    FINDGR[K]:=FIN[K]\360/6.283185;
2350    WRITE(JAK33,FORMAT1,R[K],FINDGR[K],ALFADGR[K]);
2360 END;
2370 FIMAX:=FIN[51]+1.570796;
2380 DELTAFI:=FIMAX/20;
2385 DELTAFIDGR:=DELTAFI\360/6.283185;
2390 J[51]:=J[51]*.3333;
2400 FIMAXDGR:=FIMAX\360/6.283185;
2450 WRITE (JAK33,FORMAT2);
2500 WRITE(JAK33,FORMAT1,J[51],FIMAXDGR,DELTAFIDGR);
2600 FOR N:=2 STEP 1 UNTIL 21 DO
2700    BEGIN
```

```
          FI[1]:=0;
          A3[1]:=0;
          UASR[1]:=0;
          A4[1]:=0;
          UEMSR[1]:=0;
          FI[N]:=FI[N-1]+DELTAFI;
          FIDGR[N]:=FI[N]\360/6.283185;
          FOR K:=2 STEP 1 UNTIL 51 DO
             BEGIN
                WKRN[K]:=WKR[K]\SIN(FI[N]-ALFA[2]+ALFA[K]);
                M[1]:=0;
                UA[1]:=0;
                P[1]:=0;
                UEM[1]:=0;
                IF FI[N] LSS (FIN[K]-1.570796)
                   THEN M[K]:=0
                   ELSE IF FI[N] GTR (FIN[K]+1.570796)
                      THEN M[K]:=0
                      ELSE M[K]:=1/I[51]\O[K]\SIN(FI[N]-FIN[K]+
                                    1.570796);
                CALKA3:=(M[K]+M[K-1])/2\DR;
                UA[K]:=UA[K-1]+CALKA3;
                IF FI[N] LSS (FIN[K]-1.570796)
                   THEN P[K]:=0
                   ELSE IF FI[N] GTR (FIN[K]+1.570796)
                      THEN P[K]:=0
                      ELSE P[K]:=1/I[51]\O[K]\(WKRN[K]/2550)*5\
                                   SIN(FI[N]-FIN[K]+1.570796);
                CALKA4:=(P[K]+P[K-1])/2\DR;
                UEM[K]:=UEM[K-1]+CALKA4;
             END;
                WRITE(JAK33,FORMAT1,N,FIDGR[N],UA[51],UEM[51]);
        A3[N]:=1/FIMAX\UA[51];
        A4[N]:=1/FIMAX\UEM[51];
        CALKA5:=(A3[N]+A3[N-1])/2\DELTAFI;
         UASR[N]:=UASR[N-1]+CALKA5;
        CALKA6:=(A4[N]+A4[N-1])/2\DELTAFI;
        UEMSR[N]:=UEMSR[N-1]+CALKA6;
   END;
   WRITE (JAK33,FORMAT1,UASR[21],UEMSR[21]);
   GO TO ET1;
   END.
```

APPENDIX B

In section 2 one has accepted the simplified assumption that the presence of the round-shaped sample does not change the droplet paths in the sample's neighborhood. The validity of this assumption has to be checked. Unfortunately, the solution of the equation of the droplet path for the case under consideration does not exist. There do exist, however, such solutions for the case where the droplet velocity and its direction far from the circular obstacle is equal to the gas velocity (ref. 5, 6). Let us observe, though, that in the case of a rotating sample:

1. For small droplets, where the presence of the sample may influence substantially the droplet path, the differences between the gas and the droplet velocities far from the sample are small.
2. For large droplets, these differences may be large, but the presence of the sample does not influence the droplet path.

One might expect then, that for certain convenient arrangements of parameters, one could apply an already existing solution for the case under consideration. Let us check whether this is not possible in our case.

To this end, let us establish with the aid of (ref. 6) the values of

$E \equiv \frac{y_{om}}{D_s/2}$ and φ_m (Fig. 8).

Both are functions of the parameters:

$$\kappa = \frac{2}{9} \frac{\rho_* r_*^2 w_1}{\mu \cdot D_s/2} \qquad (B1)$$

and

$$\varepsilon = \frac{18 \cdot \rho^2 \cdot D_s/2 \cdot w_1}{\mu \, \rho_*} \qquad (B2)$$

For the parameters relevant to the stand of IFFM and $w_1 = 200$ m/s, we obtain $\varepsilon = \sim 1000$ and:

r_*	10^{-6} m	5	10	20	40	60	80	100	1000
κ	--	17.2	69.0	286	915	2540	4520	6900	69000
E	--	0.830	0.920	9.977	0.990	1.0	1.0	1.0	1.0
φ_m	rad	1.450	1.515	1.540	1.560	1.564	1.566	1.568	1.5

It appears that in the case under consideration, only for droplets smaller than about $r_* = \sim 50.10^{-6}$ m, is the droplet path slightly modified in the neighborhood of the sample. For these small droplets, the application of the assumption that the droplet and gas velocity far from the obstacle does not differ significantly, seem to be fully justified.

One may apply the same reasoning as in Section 3. Then

$$\delta U_a = \frac{1}{\rho_*} \frac{\Delta M_*}{\Delta R_1} \frac{1}{\Pi D_s \sin\gamma} \frac{r_*^3 f_n(r_*, c_1) w_*(r_*, c_1)}{\int_0^\infty r_*^3 f_n(r_*, c_1) c_*(r_*, c_1) dr_*} \frac{\Delta y(r_*, c_1)}{\Delta\varphi \cdot D_s/2} \Delta r_* \qquad (B3)$$

The new elements of the nomenclature are explained in Fig. 8. Now, according to (ref. 6) one has:

$$\frac{y_o}{D_s/2} = \frac{y_{om}}{D_s/2} \left| \sin\left[\frac{\Pi}{2\varphi_m} (\varphi - \varphi_n)\right] \right| \qquad (B4)$$

Here the function $\overline{\sin}$ is defined such that

$$\left|\overline{\sin}\left[\frac{\Pi}{2\varphi_m}(\varphi-\varphi_n)\right]\right| = 0 \qquad \text{for } \varphi < \varphi_n - \varphi_m,$$

$$\left|\overline{\sin}\left[\frac{\Pi}{2\varphi_m}(\varphi-\varphi_n)\right]\right| = \left|\sin\left[\frac{\Pi}{2\varphi_m}(\varphi-\varphi_n)\right]\right| \quad \text{for } \varphi_n - \varphi_m \leq \varphi \leq \varphi_n + \varphi_m,$$

$$\left|\overline{\sin}\left[\frac{\Pi}{2\varphi_m}(\varphi-\varphi_n)\right]\right| = 0 \qquad \text{for } \varphi > \varphi_n + \varphi_m \tag{B5}$$

Hence,

$$\frac{\Delta y(r_*, c_1)}{\Delta\varphi \cdot D_s/2} = \frac{1}{D_s/2}\frac{dy_o}{d\varphi} = \frac{y_{om}}{D_s/2}\frac{\Pi}{2\varphi_m}\overline{\cos}\left[\frac{\Pi}{2\varphi_m}(\varphi-\varphi_n)\right] \tag{B6}$$

The parameters of the droplet path: $\frac{y_{om}}{D_s/2} \equiv E$, and φ_m and φ_n are functions of r_* and c_1. From (B3), (B6), and the integration of $\delta U_a(r_*, c_1, \varphi)$ extended over $0 \leq r_* \leq \infty$ results:

$$U_a(c_1,\varphi) = \frac{1}{\rho_*}\frac{\Delta M_*}{\Delta R_1}\frac{1}{\Pi D_s \sin\gamma} \cdot \int_0^\infty \frac{r_*^3 f_n(r_*,c_1)w_*(r_*,c_1)}{\int_0^\infty r_*^3 f_n(r_*,c_1)c_*(r_*,c_1)dr_*} \cdot \frac{y_{om}}{D_s/2} \cdot \frac{\Pi}{2\varphi_m} \cdot \overline{\cos}\left[\frac{\Pi}{2\varphi_m}(\varphi-\varphi_n)\right]dr_* = \frac{1}{\rho_*}\frac{\Delta M_*}{\Delta R_1}\frac{1}{\Pi D_s \sin\gamma} \cdot UA(c_1,\varphi) \tag{B7}$$

Here again the $\overline{\cos}$ function is such that

$$\overline{\cos}\left[\frac{\Pi}{2\varphi_m}(\varphi-\varphi_n)\right] = 0 \qquad \text{for } \varphi < \varphi_n - \varphi_m$$

$$\overline{\cos}\left[\frac{\Pi}{2\varphi_m}(\varphi-\varphi_n)\right] = \cos\frac{\Pi}{2\varphi_m}(\varphi-\varphi_n) \qquad \text{for } \varphi_n - \varphi_m \leq \varphi \leq \varphi_n + \varphi_m$$

$$\overline{\cos}\left[\frac{\Pi}{2\varphi_m}(\varphi-\varphi_n)\right] = 0 \qquad \text{for } \varphi > \varphi_n + \varphi_m \qquad \text{(B8)}$$

The mean value $\bar{U}_a(c_1)$ of the function $U_a(c_1,\varphi)$ calculated for $0 \leq \varphi \leq (\varphi_n+\varphi_m)_{r_{*max},c_1}$ may be obtained from:

$$\bar{U}_a(c_1) = \frac{1}{(\varphi_n+\varphi_m)_{r_{*max},c_1}} \frac{\frac{1}{\rho_*}\frac{\Delta M_*}{\Delta R_1}\frac{1}{\Pi D_s \sin\gamma}}{\int_0^\infty r_*^3 f_n(r_*,c_1)c_*(r_*,c_1)dr_*} \cdot \int_0^{(\varphi_n+\varphi_m)_{r_{*max},c_1}}$$

$$\int_0^\infty r_*^3 f_n(r_*,c_1)w_*(r_*,c_1)\frac{y_{om}}{D_s/2}\frac{\Pi}{2\varphi_m}\overline{\cos}\left[\frac{\Pi}{2\varphi_m}(\varphi-\varphi_n)\right]dr_*d\varphi$$

$$= \frac{1}{(\varphi_n+\varphi_m)_{r_{*max},c_1}} \frac{\frac{1}{\rho_*}\frac{\Delta M_*}{\Delta R_1}\frac{1}{\Pi D_s \sin\gamma}}{\int_0^\infty r_*^3 f_n(r_*,c_1)c_*(r_*,c_1)dr_*} \cdot \overline{UA}(c_1) \qquad \text{(B9)}$$

In order to calculate U_{eM} and $\overline{U}_{eM}$ one has to take into account that:

$$\frac{w_{*N}(r_*,c_1)}{w_*(r_*,c_1)} = \frac{dy_o}{d\varphi} = \frac{y_{om}}{D_s/2}\,\frac{\Pi}{2\varphi_m}\,\overline{\cos}\left[\frac{\Pi}{2\varphi_m}\,(\varphi-\varphi_n)\right] \tag{B10}$$

This relation results from the continuity equation. Hence,

$$U_{eM}(c_1,\varphi) = \frac{1}{\rho_*}\,\frac{\Delta M_*}{\Delta R_1}\,\frac{1}{\Pi\, D_s\,\sin\gamma}\cdot\int_o^\infty \frac{r_*^3\, f_n(r_*,c_1)w_*(r_*,c_1)}{\int_o^\infty r_*^3\, f_n(r_*,c_1)c_*(r_*,c_1)dr_*}\,\frac{y_{om}}{D_s/2}\,\frac{\Pi}{2\varphi_m}\cdot$$

$$\cdot\,\overline{\cos}\left[\frac{\Pi}{2\varphi_m}\,(\varphi-\varphi_n)\right]\left(\frac{w_{*N}}{2550}\right)^5 dr_* = \frac{1}{\rho_*}\,\frac{\Delta M_*}{\Delta R_1}\,\frac{1}{\Pi\, D_s\,\sin\gamma}\cdot UEM(c_1,\varphi) \tag{B11}$$

and:

$$\overline{U}_{eM}(c_1) = \frac{1}{(\varphi_n+\varphi_m)_{r_{*max},c_1}}\cdot\frac{\frac{1}{\rho_*}\,\frac{\Delta M_*}{\Delta R_1}\,\frac{1}{\Pi\, D_s\,\sin\gamma}}{\int_o^\infty r_*^3\, f_n(r_*,c_1)c_*(r_*,c_1)dr_*}\cdot\int_o^{(\varphi_n+\varphi_m)_{r_{*max},c_1}}$$

$$\int_o^\infty r_*^3\, f_n(r_*,c_1)w_*(r_*,c_1)\left(\frac{w_{*N}}{2550}\right)^5\frac{y_{om}}{D_s/2}\,\frac{\Pi}{2\varphi_m}\,\overline{\cos}\left[\frac{\Pi}{2\varphi_m}\,(\varphi-\varphi_n)\right]dr_*d\varphi$$

$$= \frac{1}{(\varphi_n+\varphi_m)_{r_{*max},c_1}}\cdot\frac{\frac{1}{\rho_*}\,\frac{\Delta M_*}{\Delta R_1}\,\frac{1}{\Pi\, D_s\,\sin\gamma}}{\int_o^\infty r_*^3\, f_n(r_*,c_1)c_*(r_*,c_1)dr_*}\cdot\overline{UEM}(c_1) \tag{B12}$$

The program of the numerical calculations is quoted below. It provides also the possibility to calculate the mean values of the impact velocity. The following mean values have been introduced:

$$\bar{w}_{*N_{AR}}(c_1,\varphi) = \int_0^\infty w_{*N}(r_*,c_1,\varphi)\, f_n(r_*,c_1)dr_* \Big/ \int_0^\infty f_n(r_*,c_1)dr_* \qquad (B9)$$

$$\bar{w}_{*N_{M}}(c_1,\varphi) = \int_0^\infty w_{*N}(r_*,c_1,\varphi) r_*^3\, f_n(r_*,c_1)dr_* \Big/ \int_0^\infty r_*^3\, f_n(r_*,c_1)dr_* \qquad (B10)$$

and

$$\bar{\bar{w}}_{*N_{AR}}(c_1) = \frac{1}{(\varphi_n+\varphi_m)_{r_{*max}}} \int_0^{(\varphi_n+\varphi_m)_{r_{*max}}} \bar{w}_{*N_{AR}}(c_1,\varphi)d\varphi \qquad (B11)$$

$$\bar{\bar{w}}_{*N_{M}}(c_1) = \frac{1}{(\varphi_n+\varphi_m)_{r_{*max}}} \int_0^{(\varphi_n+\varphi_m)_{r_{*max}}} \bar{w}_{*N_{M}}(c_1,\varphi)d\varphi \qquad (B12)$$

The numerical calculations were performed for the same group of parameters as in Section 4. The results are shown also in that section. The input data have to be sequenced according to the sequence numbers: 900, 1000, 1004, where:

$c_1 \equiv C1$, $u \equiv U$, $\gamma \equiv GAMA$, $D_s/2 \equiv RP$, the amount of terms in the (r_*)-array $\equiv Z1$, (φ)-array $\equiv Z2$, (κ, E, φ_m)-array $\equiv Z3$, respectively, $\Delta r_* \equiv DR$, $\mu \equiv MI$, $\rho \equiv RO$, $\rho_* \equiv RO1$, $z \equiv Z$, $N_1 \equiv N11$, $N_2 \equiv N22$, $N_3 \equiv N33$, array: $(\kappa \equiv KB1[S]$, $E \equiv E1[S]$, $\varphi_m \equiv FIM1[S])$ for $1 \leq S \leq Z3$,

The array (κ, E, φ_m) called JAK1 may be stored either on tape or in the memory of the computer. It is being put into the program in accordance with the sequence number 1004.

The output data are being printed in the sequence resulting from sequence numbers: 2350, 2500, 5050, and 5800 where:

$r_* \equiv R[K]$, $\varphi_n(r_*, c_1) \equiv FINDGR[K]$, $\alpha(r_*, c_1) \equiv ALFADGR[K]$, $\kappa(r_*, c_1) \equiv KB[K]$,

$E(r_*, c_1) \equiv E[K]$, $\varphi_m(r_*, c_1) \equiv FIM[K]$, $r_{*m} \equiv J[Z1]$, $(\varphi_n + \varphi_m)_{r_{*max}} \equiv FIMAXDGR$,

$\Delta\varphi = \dfrac{(\varphi_n + \varphi_m) r_{*max}}{Z2-1} \equiv DELTAFIDGR$, N, $\varphi[N] \equiv FIDGR[N]$, $UA(c_1, \varphi) \equiv UA[Z1]$,

$UEM(c_1, \varphi) \equiv UEM[Z1]$, $\overline{w}_{*N_{AR}}(C_1, \varphi) \equiv WKRNAR[Z1]$, $\overline{w}_{*N_M}(c_1, \varphi) \equiv WKRNMAS[Z1]$,

$\overline{UA}(c_1) \equiv UASR[Z2]$, $\overline{UEM}(c_1) \equiv UEMSR[Z2]$, $\overline{\overline{w}}_{*N_{AR}}(c_1) \equiv WKRNARSR[Z2]$, $\overline{\overline{w}}_{*N_M}(c_1) \equiv$ WKRNMASSR[Z2].

```
100   BEGIN
200   COMMENT BADANIE UA,UEM DLA WIRUJACEJ PROBKI W FUNKCJI C1 (WARIII);
300   REAL C1,U,GAMA,N11,N22,N33,DR,MI,RO,RO1,Z,CALKA1,CALKA2,
350         FIMAX,DELTAFI,FIMAXDGR,DELTAFIDGR,CALKA3,CALKA4,
360          CALKA5,CALKA6,CALKA7,CALKA8,CALKA9,CALKA10,RP;
400   INTEGER K,N,S,T,Z1,Z2,Z3;
500   LABEL ET1,ET2,ET3,ET4,ET5;
600   ARRAY R,FN,A1,CKR,H,I,G,J,L,WKR,M,O,UA,P,UEM,
650          TGALFA,ALFA,FIN,ALFADGR,FINDGR,WKRN,
655           Q1,WKRNAR,Q2,WKRNMAS,KB,FIM,E[1:300],
660          A3,A4,UASR,UEMSR,FI,FIDGR,A5,A6,WKRNARSR,WKRNMASSR[1:200],
670           KB1,E1,FIM1[1:100];
700   FILE JAK33 REMOTE(2,9);
710   FILE JAK1 DISK SERIAL (2,10,30);
800   FORMAT FORMAT1 (6E11.3);
850   FORMAT FORMAT2(X1);
900   ET1: READ(JAK33,/,C1,U,GAMA,RP,Z1,Z2,Z3,DR,MI,RO,RO1,Z);
1000 READ (JAK33,/,N11,N22,N33);
1001  FOR S:=1 STEP 1 UNTIL Z3 DO
1002  BEGIN
1004   READ (JAK1,/,KB1[S],E1[S],FIM1[S]);
1005  END;
1010 CALKA1:=0;
1020 CALKA2:=0;
1100 K:=2;
1200 R[K-1]:=0;
1205 G[K-1]:=0;
1210 H[K-1]:=0;
1220 I[K-1]:=0;
1230 J[K-1]:=0;
1300 FOR K:=2 STEP 1 UNTIL Z1 DO
1400  BEGIN
1500    R[K]:=R[K-1]+DR;
1600    FN[K]:=N11\R[K]*N22\EXP(-N33\R[K]);
1700    A1[K]:=SQRT((.85\MI\RO)/(R[K]*3\RO1*2\C1));
1800    CKR[K]:=.8\C1\(1-1/(1+A1[K]\Z+
1900             SQRT(A1[K]*2\Z*2+2\A1[K]\Z))*2);
1910    WKR[K]:=SQRT(U*2\(SIN(GAMA))*2+(CKR[K]-U\COS(GAMA))*2);
1915    KB[K]:=(2\1000\R[K]*2\WKR[K])/(9\MI\RP);
1920    T:=0;
1925    ET2: T:=T+1;
1930         IF KB[K] GTR KB1[T] THEN GO TO ET3;
1935    ET3: IF KB[K] LSS KB1[T+1] THEN
1940          E[K]:=(E1[T+1]-E1[T])/(KB1[T+1]-KB1[T])\
1945                (KB[K]-KB1[T])+E1[T]
1960         ELSE GO TO ET2;
1965     T:=0;
1970     ET4: T:=T+1;
1975          IF KB[K] GTR KB1[T] THEN GO TO ET5;
1980     ET5: IF KB[K] LSS KB1[T+1] THEN
1985          FIM[K]:=(FIM1[T+1]-FIM1[T])/(KB1[T+1]-KB1[T])\
1990                (KB[K]-KB1[T])+FIM1[T]
1995          ELSE GO TO ET4;
2000    G[K]:=R[K]*3\FN[K];
2050    H[K]:=R[K]*3\CKR[K]\FN[K];
2055     O[K]:=R[K]*3\WKR[K]\FN[K];
```

```
2100     CALKA1:=(H[K-1]+H[K])/2\DR;
2200     I[K]:=I[K-1]+CALKA1;
2300     CALKA2:=(G[K-1]+G[K])/2\DR;
2310     J[K]:=J[K-1]+CALKA2;
2320     TGALFA[K]:=SIGN(SIN((CKR[K]-U\COS(GAMA))/WKR[K]))\
2323                WKR[K]/(U\SIN(GAMA))\SQRT(1-U*2\(SIN(GAMA))*2/
2326                WKR[K]*2);
2330     ALFA[K]:=ARCTAN(TGALFA[K]);
2333     IF K EQL 2
2336        THEN FIN[K]:=1.570796
2339        ELSE FIN[K]:=FIN[K-1]+ALFA[K-1]-ALFA[K];
2340     ALFADGR[K]:=ALFA[K]\360/6.283185;
2345     FINDGR[K]:=FIN[K]\360/6.283185;
2350      WRITE(JAK33,FORMAT1,R[K],FINDGR[K],ALFADGR[K],
2355            KB[K],E[K],FIN[K]);
2360 END;
2370 FIMAX:=FIN[Z1]+FIM[Z1];
2380  DELTAFI:=FIMAX/(Z2-1);
2385 DELTAFIDGR:=DELTAFI\360/6.283185;
2390  J[Z1]:=J[Z1]*.3333;
2400 FIMAXDGR:=FIMAX\360/6.283185;
2450 WRITE (JAK33,FORMAT2);
2500 WRITE(JAK33,FORMAT1,J[Z1],FIMAXDGR,DELTAFIDGR);
2600 FOR N:=2 STEP 1 UNTIL Z2 DO
2700     BEGIN
2701       FI[1]:=0;
2702       A3[1]:=0;
2704       UASR[1]:=0;
2706       A4[1]:=0;
2708       UEMSR[1]:=0;
2710       A5[1]:=0;
2712       WKRNARSR[1]:=0;
2714       A6[1]:=0;
2716       WKRNMASSR[1]:=0;
2800       FI[N]:=FI[N-1]+DELTAFI;
2850       FIDGR[N]:=FI[N]\360/6.283185;
2900       FOR K:=2 STEP 1 UNTIL Z1 DO
3000         BEGIN
3100            IF FI[N] LSS (FIN[K]-FIM[K])
3110               THEN WKRN[K]:=0
3120               ELSE IF FI[N] GTR (FIN[K]+FIM[K])
3130                 THEN WKRN[K]:=0
3140                 ELSE WKRN[K]:=WKR[K]\E[K]\1.570796/FIM[K]
3150                             \COS(1.570796/FIM[K]\(FI[N]-
3155                               FIN[K]));
3200           M[1]:=0;
3210           UA[1]:=0;
3250           P[1]:=0;
3260           UEM[1]:=0;
3265            Q1[1]:=0;
3270            WKRNAR[1]:=0;
3275            Q2[1]:=0;
3280            WKRNMAS[1]:=0;
3300           IF FI[N] LSS (FIN[K]-FIM[K])
3400             THEN M[K]:=0
3500             ELSE IF FI[N] GTR (FIN[K]+FIM[K])
```

```
3600                    THEN M[K]:=0
3700                     ELSE M[K]:=1/I[Z1]\O[K]\E[K]\1.570796/FIM[K]
3800                              \COS(1.570796/FIM[K]\(FI[N]-FIN[K]));
3900                CALKA3:=(M[K]+M[K-1])/2\DR;
4000                UA[K]:=UA[K-1]+CALKA3;
4100                IF FI[N] LSS (FIN[K]-FIM[K])
4200                  THEN P[K]:=0
4300                  ELSE IF FI[N] GTR (FIN[K]+FIM[K])
4400                    THEN P[K]:=0
4500                     ELSE P[K]:=1/I[Z1]\O[K]\E[K]\1.570796/FIM[K]
4550                              \COS(1.570796/FIM[K]\(FI[N]-FIN[K]))
4600                              \(WKRN[K]/2550)*5;
4700                CALKA4:=(P[K]+P[K-1])/2\DR;
4800                UEM[K]:=UEM[K-1]+CALKA4;
4810                 Q1[K]:=WKRN[K]\FN[K];
4820                 CALKA7:=(Q1[K]+Q1[K-1])/2\DR;
4830                 WKRNAR[K]:=WKRNAR[K-1]+CALKA7;
4840                 Q2[K]:=WKRN[K]\R[K]*3\FN[K];
4850                 CALKA8:=(Q2[K]+Q2[K-1])/2\DR/J[Z1]*3;
4960                 WKRNMAS[K]:=WKRNMAS[K-1]+CALKA8;
5000              END;
5050                WRITE(JAK33,FORMAT1,N,FIDGR[N],UA[Z1],UEM[Z1],
5055                      WKRNAR[Z1],WKRNMAS[Z1]);
5100          A3[N]:=1/FIMAX\UA[Z1];
5200          A4[N]:=1/FIMAX\UEM[Z1];
5300          CALKA5:=(A3[N]+A3[N-1])/2\DELTAFI;
5400           UASR[N]:=UASR[N-1]+CALKA5;
5500          CALKA6:=(A4[N]+A4[N-1])/2\DELTAFI;
5600          UEMSR[N]:=UEMSR[N-1]+CALKA6;
5610           A5[N]:=1/FIMAX\WKRNAR[Z1];
5620           A6[N]:=1/FIMAX\WKRNMAS[Z1];
5630           CALKA9:=(A5[N]+A5[N-1])/2\DELTAFI;
5640           WKRNARSR[N]:=WKRNARSR[N-1]+CALKA9;
5650           CALKA10:=(A6[N]+A6[N-1])/2\DELTAFI;
5660           WKRNMASSR[N]:=WKRNMASSR[N-1]+CALKA10;
5700   END;
5800   WRITE (JAK33,FORMAT1,UASR[Z2],UEMSR[Z2],WKRNARSR[Z2],
5850          WKRNMASSR[Z2]);
5900   GO TO ET1;
6000   END.
```

```
P JAK1
100    8,
200    17.1,  0.830,  1.45,
300    68.4,    0.920,  1.515,
400    274,     0.977,  1.540,
500    1095,    0.990,  1.560,
600    2460,    1.0,    1.564,
700    4380,    1.0,    1.566,
800    6840,    1.0,    1.568,
900    684000,  1.0,    1.570,
```

8. REFERENCES

1. J. Krzyżanowski, "The Correlation Between Droplet Stream Structure and Steam Turbine Blading Erosion," Technical Report No. 147, Department of Mechanical and Aerospace Engineering, University of Delaware, December, 1971.

2. W. D. Pouchot, F. J. Heymann, et al, "Basic Investigation of Turbine Erosion Phenomena," NASA Contractor Report, NASA C 1830, November, 1971.

3. B. Weigle, H. Severin, "The Investigation of the Relationship Between the Gas Velocity, the Droplet Stream Structure and the Erosion Rate-Time Pattern," (in Polish), Report of IFFM, No. 273/71, Gdańsk, Poland, December, 1971.

4. F. J. Heymann, "Toward Quantitative Prediction of Liquid Impact Erosion," ASTM STP 474, American Society of Testing and Materials, pp. 212-248, 1970.

5. G. Gyarmathy, "Foundation of the Theory of Wet-Steam Turbine," (in German), Juris-Verlag, Zurich, 1960.

6. R. J. Brun, W. Lewis, P. J. Perkins, J. S. Serafini, "Impingement of Cloud Droplets on a Cylinder and Procedure for Measuring Liquid-Water Contents and Droplet Size Supercooled Clouds by Rotating Multi-cylinder Method," NAS Report No. 125, 1955.

9. LIST OF FIGURES

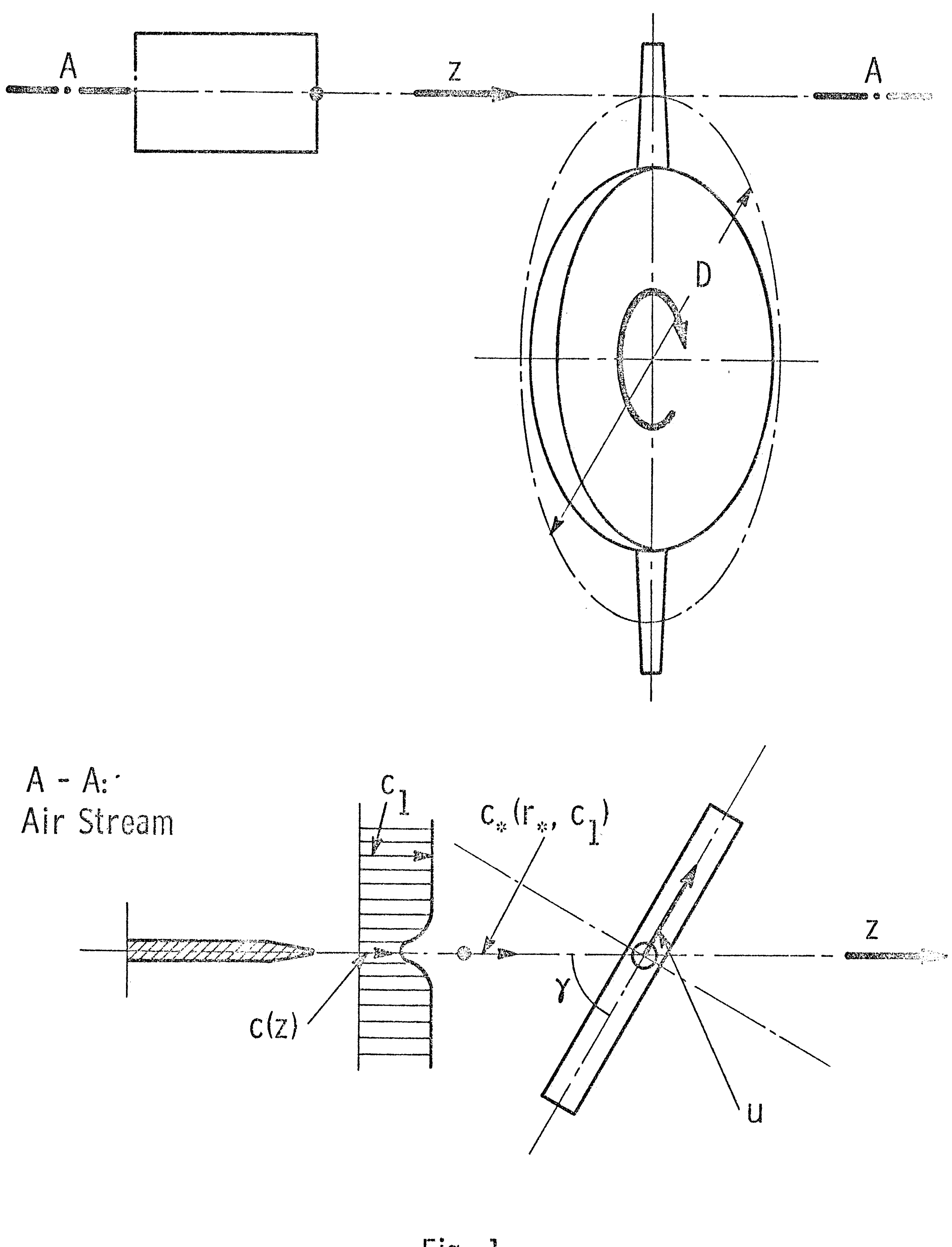

Fig. 1

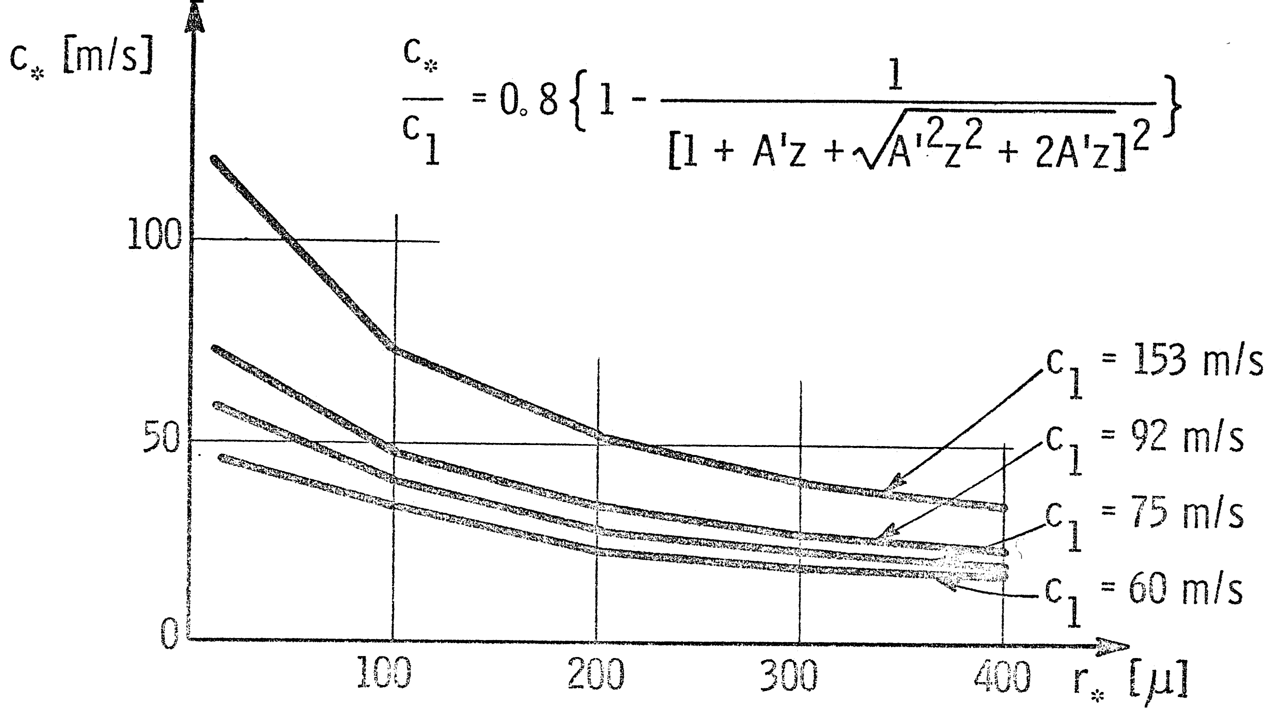

$$\frac{c_*}{c_1} = 0.8\left\{1 - \frac{1}{[1 + A'z + \sqrt{A'^2z^2 + 2A'z}]^2}\right\}$$

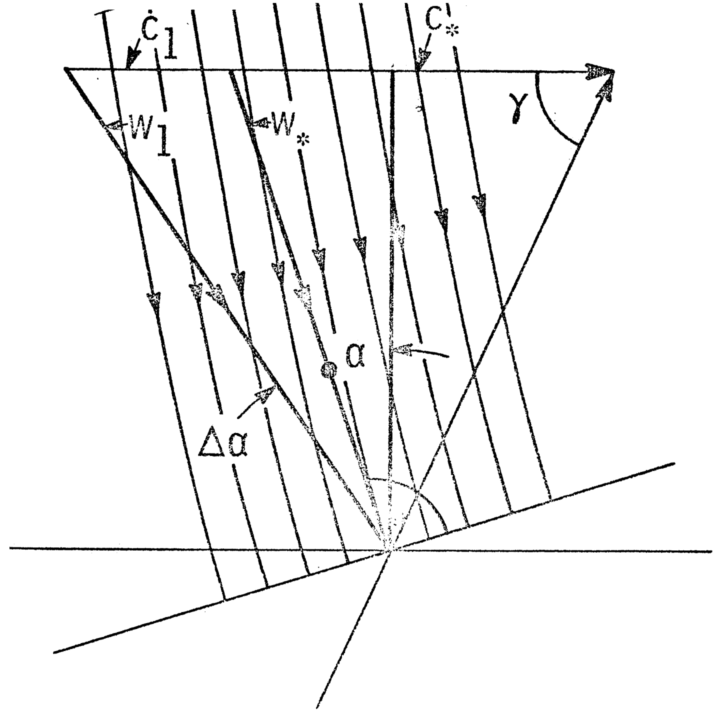

$$A' = \sqrt{\frac{0.85\,\mu\rho}{r_*^3\,\rho_*^2\,c_1}}$$

$u = 200$ m/s

$\gamma = 80^0$

$D_s = 7 \cdot 10^{-3}$ m

$\mu = 1.85 \cdot 10^{-5}$ kg/ms

$\rho = 1.205$ kg/m^3

$\rho_* = 1000$ kg/m^3

$z = 0.3$ m

c_1	m/s	60		75		92		153	
r_*	μ	10	400	10	400	10	400	10	400
w_1	m/s	198.5		199.0		200.5		220.0	
w_*	m/s	197.5	197.5	198.5	197.5	200.5	197.0	214.5	197.0
α	0	+ 3°42'	- 5°14'	+ 7°06'	- 4°39'	+10°55'	- 3°38'	+23°32'	- 0°30'
Δα	0	3°57'	13°53'	2°00'	13°45'	6°45'	20°18'	7°48'	31°50'

Fig. 2

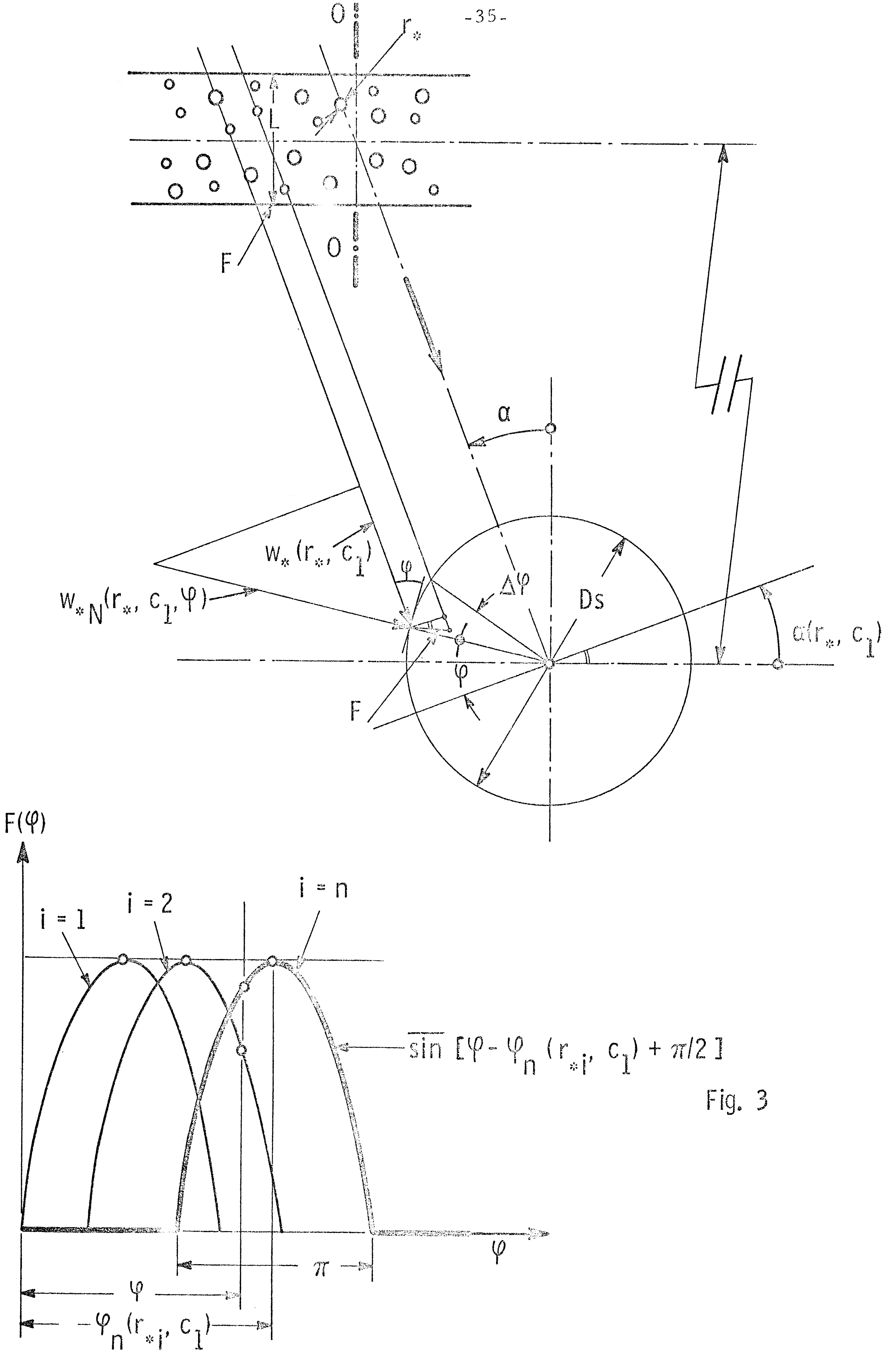
O
r*
L
O
F
α
w*(r*, c1)
φ
w*N(r*, c1, φ)
Δφ
Ds
α(r*, c1)
φ
F
F(φ)
i = 1
i = 2
i = n
sin [φ - φn (r*i, c1) + π/2]
φ
π
φ
φn(r*i, c1)

Fig. 3

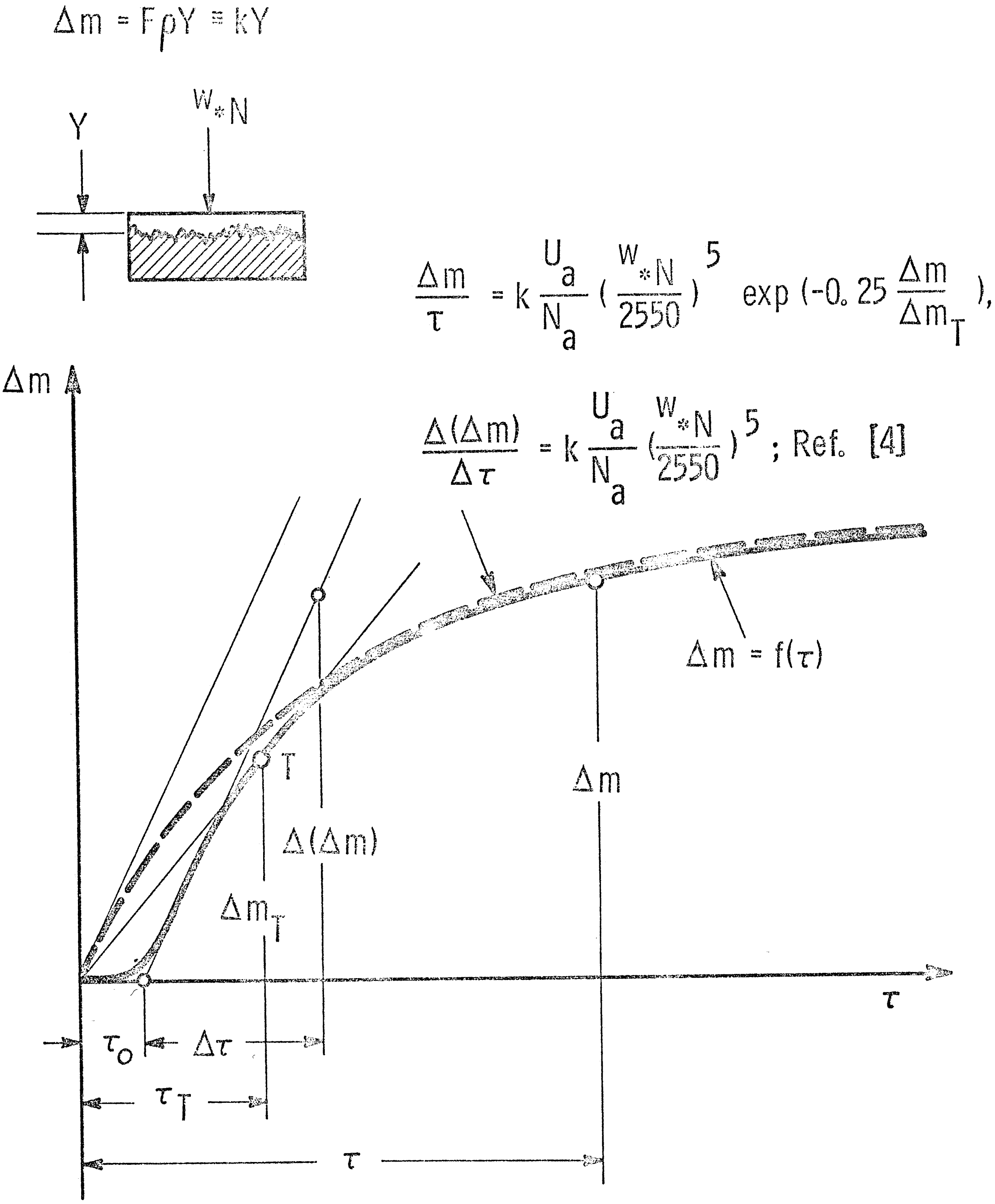

$\Delta m = F\rho Y \equiv kY$
Y
$w_* N$
$\frac{\Delta m}{\tau} = k \frac{U_a}{N_a} \left(\frac{w_* N}{2550} \right)^5 \exp\left(-0.25 \frac{\Delta m}{\Delta m_T}\right),$
Δm
$\frac{\Delta(\Delta m)}{\Delta \tau} = k \frac{U_a}{N_a} \left(\frac{w_* N}{2550} \right)^5$; Ref. [4]
Δm = f(τ)
T
Δm
Δ(Δm)
Δm_T
τ
τ_o
Δτ
τ_T
τ

Fig. 4

Fig. 5

a)

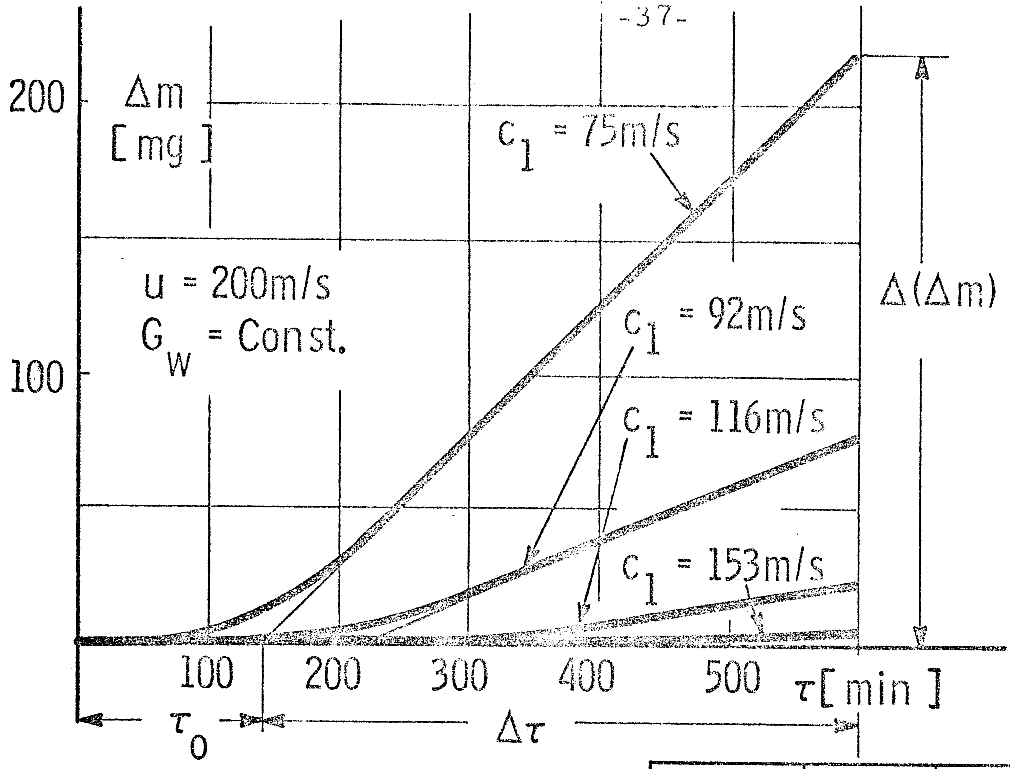

c_1 m/s	75	92	116	153	m/s
$\frac{\Delta(\Delta m)}{\Delta\tau}$	0.482	0.199	0.076	0.020	mg/min
τ_0	143	222	318	374	min

b)

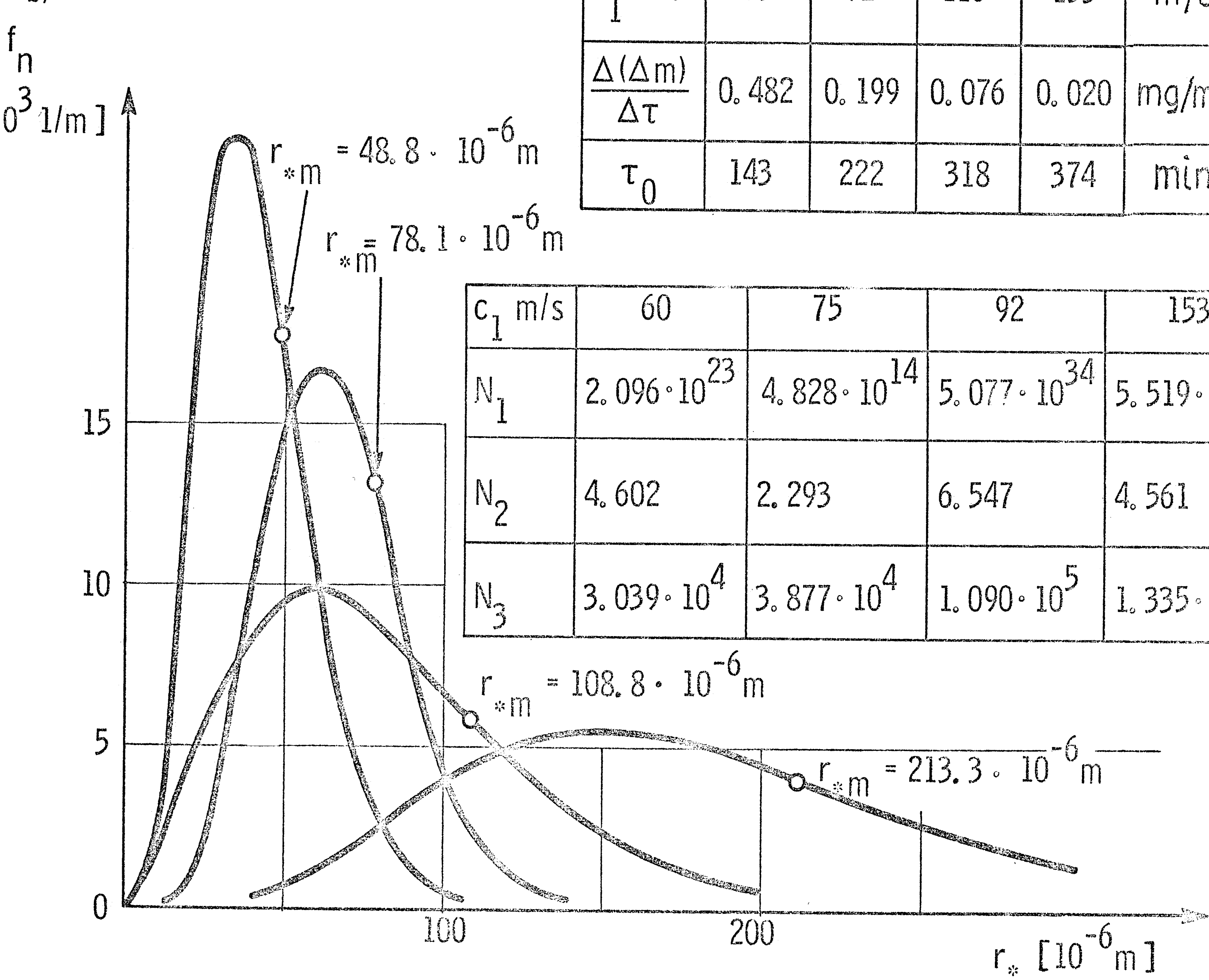

c_1 m/s	60	75	92	153
N_1	$2.096 \cdot 10^{23}$	$4.828 \cdot 10^{14}$	$5.077 \cdot 10^{34}$	$5.519 \cdot 10^{2}$
N_2	4.602	2.293	6.547	4.561
N_3	$3.039 \cdot 10^{4}$	$3.877 \cdot 10^{4}$	$1.090 \cdot 10^{5}$	$1.335 \cdot 10^{5}$

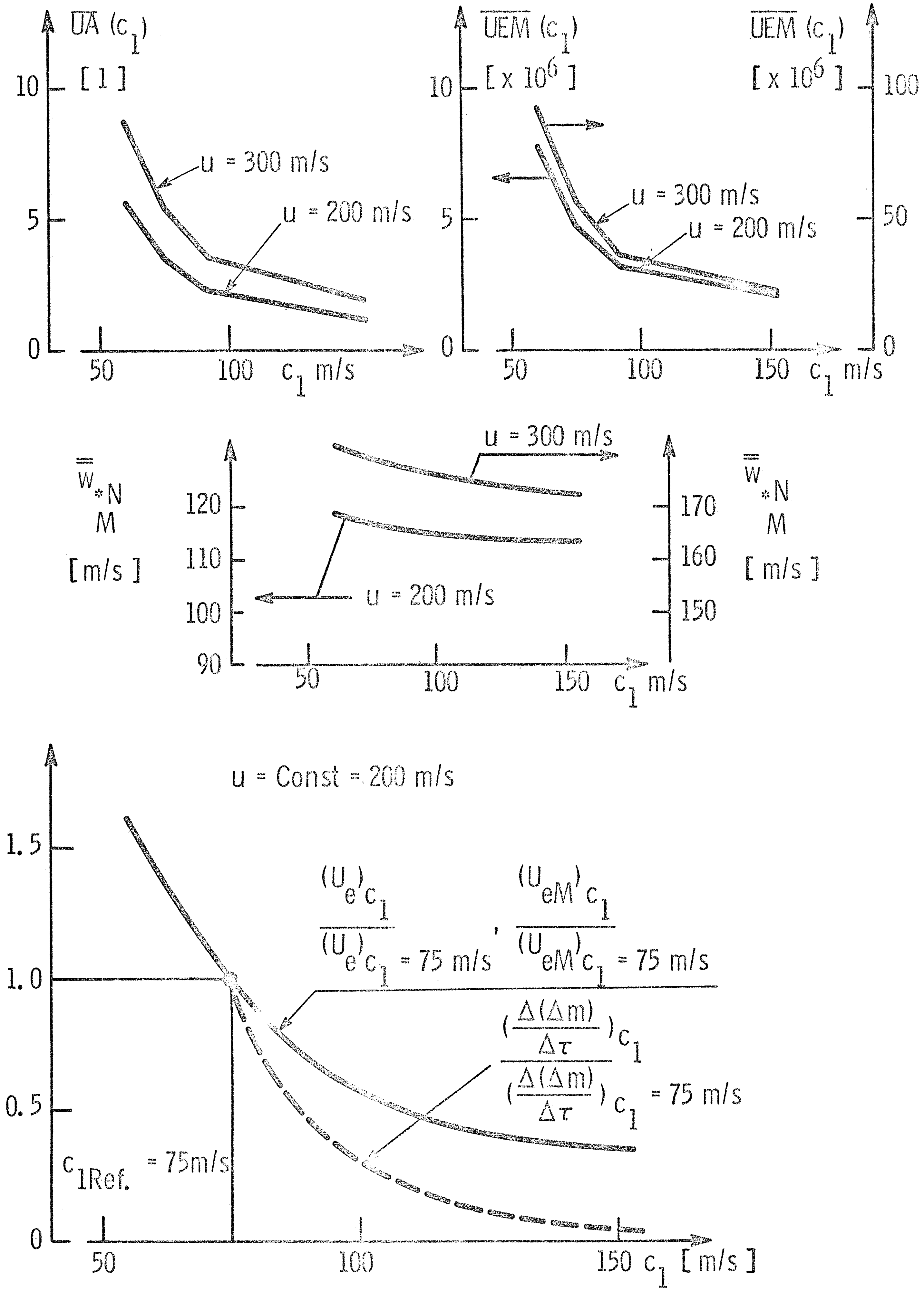

$\overline{UA}$ (c_1)
[1]
10
5
0
u = 300 m/s
u = 200 m/s
50
100
c_1 m/s
$\overline{UEM}$ (c_1)
[x 10^6]
10
5
0
u = 300 m/s
u = 200 m/s
50
100
150
c_1 m/s
$\overline{UEM}$ (c_1)
[x 10^6]
100
50
0
$\overline{\overline{w}}_{*N}$ M
[m/s]
120
110
100
90
u = 300 m/s
u = 200 m/s
50
100
150
c_1 m/s
170
160
150
$\overline{\overline{w}}_{*N}$ M
[m/s]
u = Const = 200 m/s
1.5
1.0
0.5
0
$\frac{(U_e)_{c_1}}{(U_e)_{c_1 = 75\ m/s}}$, $\frac{(U_{eM})_{c_1}}{(U_{eM})_{c_1 = 75\ m/s}}$
$\frac{(\frac{\Delta(\Delta m)}{\Delta \tau})_{c_1}}{(\frac{\Delta(\Delta m)}{\Delta \tau})_{c_1 = 75\ m/s}}$
$c_{1Ref.}$ = 75m/s
50
100
150
c_1 [m/s]

Fig. 6

Fig. 7

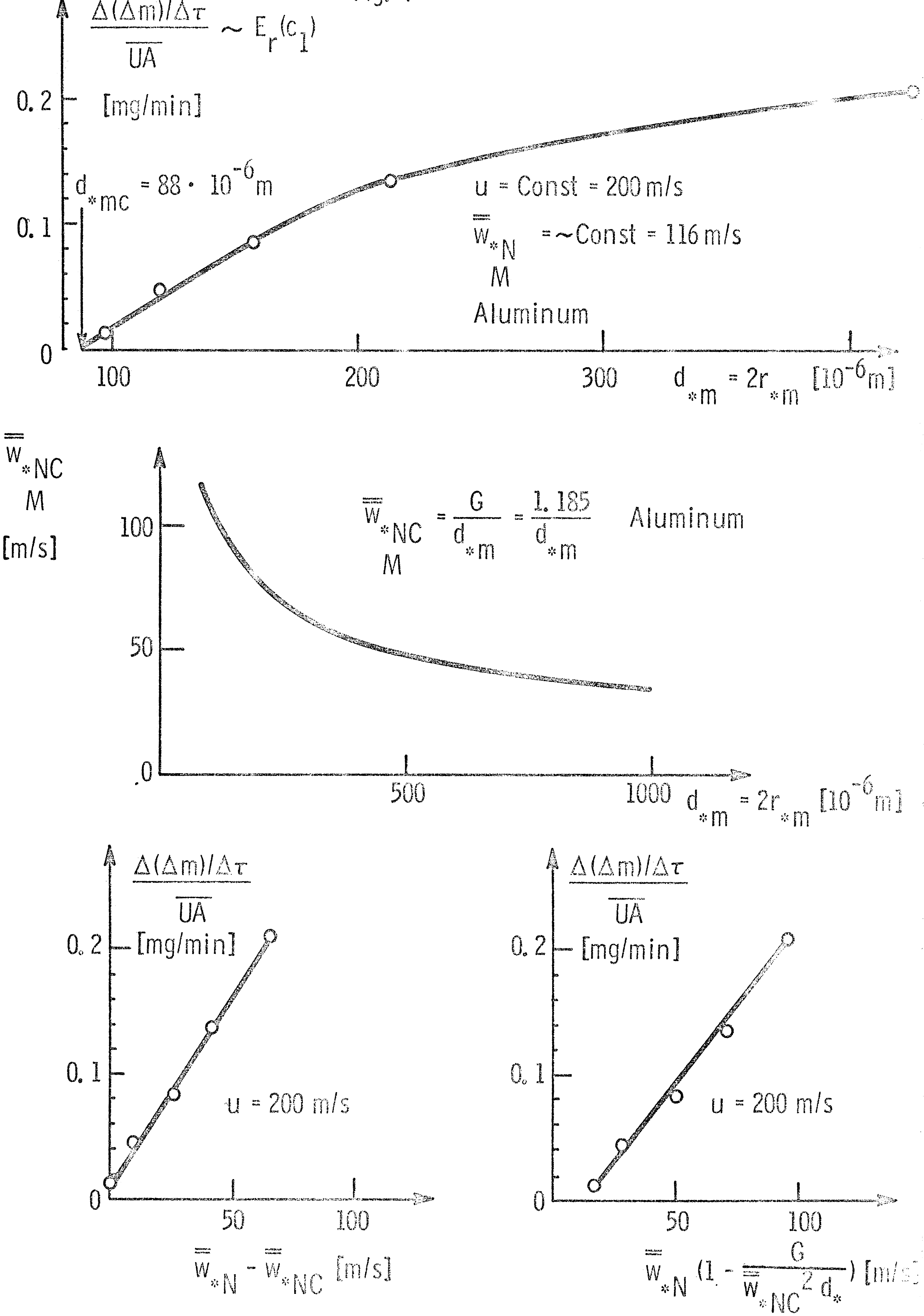
Δ(Δm)/Δτ / UA ~ E_r(c_1)
[mg/min]
0.2
0.1
0
d_*mc = 88 · 10^-6 m
u = Const = 200 m/s
w_*N M = ~Const = 116 m/s
Aluminum
100
200
300
d_*m = 2r_*m [10^-6 m]
w_*NC M
[m/s]
100
50
0
w_*NC M = G / d_*m = 1.185 / d_*m
Aluminum
500
1000
d_*m = 2r_*m [10^-6 m]
Δ(Δm)/Δτ / UA
[mg/min]
0.2
0.1
0
u = 200 m/s
50
100
w_*N - w_*NC [m/s]
Δ(Δm)/Δτ / UA
[mg/min]
0.2
0.1
0
u = 200 m/s
50
100
w_*N (1 - G / w_*NC^2 d_*) [m/s]

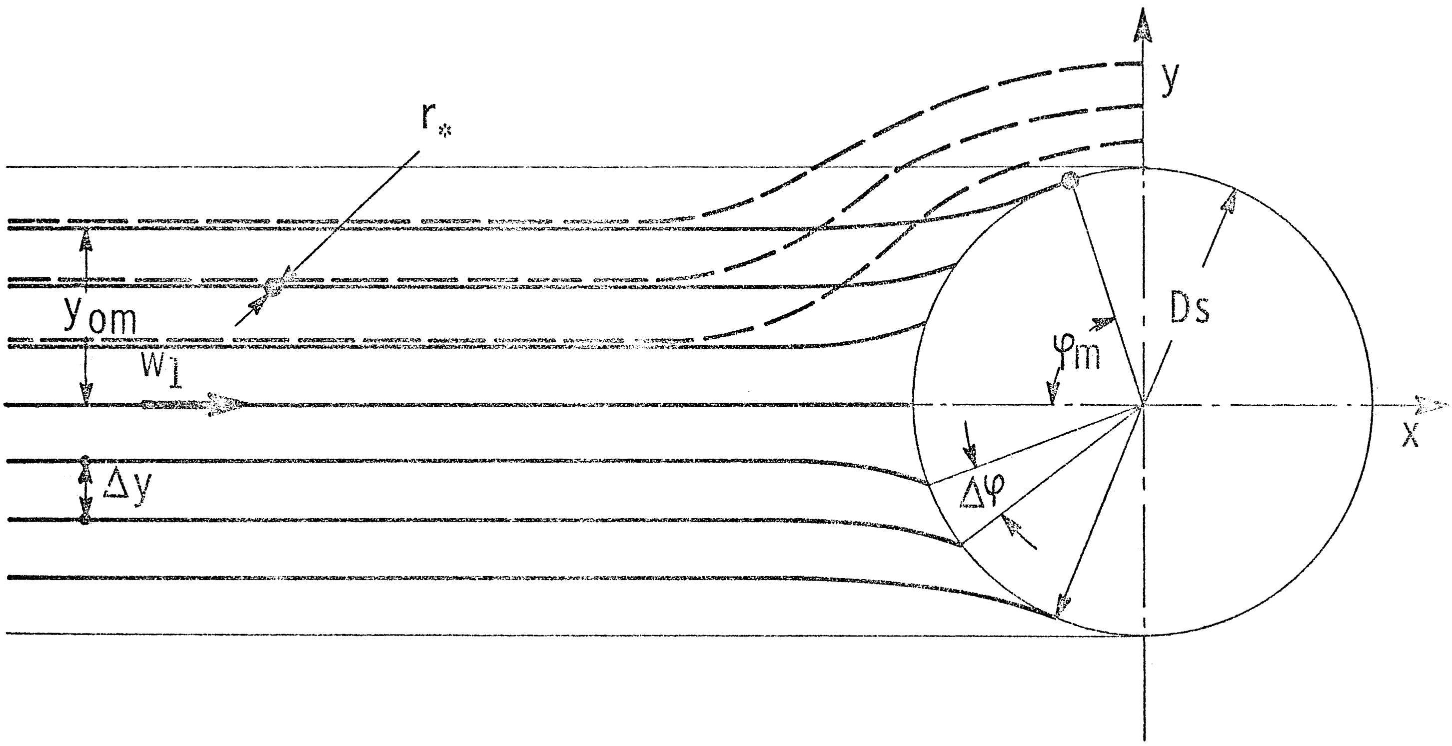

Fig. 8